J. Chem. Sci. Vol. 128, No. 7, July 2016, pp. 1119–1130.
DOI 10.1007/s12039-016-1104-2

Ba/ZrO_2 nanoparticles as efficient heterogeneous base catalyst for the synthesis of β-nitro alcohols and 2-amino 2-chromenes

SAGNIKA PRADHAN, KUMARI SWARNIMA and B G MISHRA*
Department of Chemistry, National Institute of Technology, Rourkela, Odisha 769 008, India
e-mail: brajam@nitrkl.ac.in

MS received 11 February 2016; revised 26 March 2016; accepted 3 May 2016

Abstract. Zirconia nanoparticles were synthesized by precipitation, urea hydrolysis, amorphous citrate and combustion synthesis methods. The zirconia surface was subsequently modified by grafting Ba^{2+} species. The Ba^{2+} modified zirconia (Ba/ZrO_2) materials were characterized using XRD, Fourier analysis, UV-vis-DRS, FESEM and HRTEM techniques. XRD study indicated selective stabilization of the tetragonal phase of zirconia in the presence of Ba^{2+} species. Fourier line profile analysis of the XRD peaks revealed that the average crystallite size of the zirconia nanoparticles is in the range of 5-15 nm. The surface area, basicity and barium content of the material depend strongly on the method of synthesis. The Ba/ZrO_2 catalyst prepared by urea hydrolysis method exhibited higher surface area and barium content compared to other samples. The catalytic activity of the Ba/ZrO_2 catalyst was evaluated for synthesis of β-nitro alcohols and 2-amino 2-chromenes. The β-nitro alcohols were synthesized by condensation of aryl aldehydes and nitromethane. Similarly, the 2-amino 2-chromenes were synthesized by condensation of arylaldehydes, α-naphthol and malononitrile. The Ba/ZrO_2 catalyst was found to be highly efficient for synthesis of both classes of compounds providing excellent yield and purity of the products.

Keywords. Urea hydrolysis; amorphous citrate method; combustion synthesis; β-nitro alcohols; 2-amino 2-chromenes.

1. Introduction

Heterogeneous-base catalyzed organic synthesis is a promising field of research with potential application in pharmaceuticals and related fine chemical industries.[1–5] Among different heterogeneous base catalysts studied for fine chemical synthesis, the alkali and alkaline earth metal oxides are quite promising because they are inexpensive, easy to prepare and display strong surface basic sites capable of promoting a variety of base catalyzed reactions.[1–3] However, the low surface area and loss of active sites due to surface passivation are the important factors which limit their application in base catalyzed processes. The stability of the active sites of these materials can be improved by forming nanocomposites with a suitable second oxide component.[2–7] Zirconia by virtue of its high thermal stability, extreme hardness, stability under reducing conditions, and surface acidic and basic functions is ideal candidate for preparation of composite catalytic materials. The surface and structural modification of zirconia has been carried out to prepare several promising catalytic materials such as CeO_2-ZrO_2 and SO_4^{2-}/ZrO_2.[8,9] Recently, a series of zirconia-based alkali and alkaline earth metal oxide nanocomposite materials such as ZrO_2-CaO, ZrO_2-MgO, Na-incorporated mesoporous zirconia, Cs^+ exchanged nanozironia have been studied as catalyst for base catalyzed reactions.[10–17] The Ca^{2+} ions substitute for Zr^{4+} ions in zirconia lattice to form a solid solution. The CaO-ZrO_2 solid solution exhibit oxygen ion vacancy and increased iconicity of the zirconia lattice resulting in formation of new basic sites.[7–9] Similarly, the presence of MgO stabilizes the tetragonal phase of zirconia and helps creating new basic sites in the host zirconia lattice which are resistant to deactivation by hydrolysis.[10–12] Recently, sodium incorporated mesoporous zirconia has been synthesized by hard templating approach which exhibit tetragonal crystalline frameworks, superbasicity (27.0 in Hammet scale) and excellent catalytic activity for synthesis of dimethyl carbonate.[16] Zirconia nanoparticles, when synthesized in hydrous form, contain a significant fraction of reactive hydroxyl groups on its surface. These hydroxyl groups can act as anchoring sites for catalytically active species. Essayem *et al*., have synthesized Cs^+ exchanged zirocnia nanoparticles by ion exchange method. The Cs^+ ions are bonded to the surface of zirconia by electrostatic forces and serve as excellent basic sites due to charge isolation.[17] The literature studies clearly indicate that the surface and structural modification of

*For correspondence

zirconia nanoparticles by alkali and alkaline earth metal can generate novel heterogeneous base catalyst for fine chemical synthesis. With an intention to develop novel heterogeneous basic catalyst, in this work, we have prepared Ba^{2+} modified zirconia nanoparticles. The zirconia nanoparticles were synthesized using four different routes and subsequent grafting of the Ba^{2+} ions was performed by treatment of barium carbonate precursor salt solution. The catalytic activity of the Ba/ZrO_2 material has been evaluated for synthesis of β-nitroalcohols and 2-amino 2-chromenes.

The Henry (nitroaldol condensation) reaction is a significant C–C bond formation reaction which involves the synthesis of β-nitro alcohol by condensation of aryl aldehydes and nitroalkanes.[18] Since many natural products contain nitrogen atoms, the Henry reaction provides a basis for development of such molecules. The β-nitro alcohol synthesized by the Henry reaction route is used as an intermediate for the synthesis of β-amino alcohol, amino sugar, ketones, pyrroles, porphyrins and pharmacologically potent compounds.[18,19] Various homogeneous and heterogeneous catalytic systems studied for this reaction include amine-MCM-41 hybrids, MCM-41-Cu(salen) complex, I_2/K_2CO_3, polyamine functionalized mesoporous zirconia, silica-supported amine catalysts, and CsF/[bmim][BF_4] ionic liquids.[20–23] Many of the reported method employ homogeneous catalyst, supported reagents or covalently grafted organic bases which suffer from various issues such as catalyst stability, recyclability, regeneration and harsh reaction condition. It is therefore highly desirable to develop novel catalytic protocols using heterogeneous base catalysts which are stable, inexpensive, and recyclable, which can catalyze the β-nitro alcohol formation reaction under mild conditions.

Synthesis of 2-amino 2-chromenes and their modified analogues is of significant interest in organic synthesis because of their potential applications as cosmetics, pigments, potential agrochemicals.[24,25] The aminochromene motifs are found as a structural constituent in many natural products of biological significance.[25,26] The multicomponent condensation reaction of aldehyde, malononitrile, and activated phenol has recently emerged as a promising route for synthesis of structurally diverse 2-amino 2-chromene.[4,5,25–27] The proper choice of the reaction media and catalytic system is crucial for expeditious synthesis of 2-amino 2-chromene.[4] Various synthetic methods developed in literature towards synthesis of this class of biologically important compounds include the $Na_2CaP_2O_7$, basic alumina, Silica-supported piperazine, 4-dimethylaminopyridine functionalized polyacrylonitrile fiber catalyst, basic ionic liquid as catalyst/reagent.[26–33] However, most of the reported methods require longer reaction time, involve stoichiometric reagents, and toxic solvents, with moderate yields of the product. In this work, we have utilized the Ba/ZrO_2 material as an efficient heterogeneous catalyst for synthesis of structurally diverse 2-amino 2-chromenes in water + PEG (1:1) mixed reaction media.

2. Experimental

2.1 *Materials and methods*

Zirconyl nitrate [$ZrO(NO_3)_2.xH_2O$], zirconyl chloride [$ZrOCl_2.8H_2O$], urea [CH_4N_2O], citric acid [$C_6H_8O_7$] and liquid ammonia were obtained from Merck India Pvt. Ltd. All chemicals were of analytical reagent grade and used directly without further purification. Double distilled water prepared in the laboratory was used in the preparation process.

2.2 *Synthesis of zirconia nanoparticles*

The zirconia particles were synthesized using four different methods namely precipitation, urea hydrolysis, amorphous citrate, and combustion synthesis methods. The detail scheme elucidating the synthetic procedure adopted for preparation of zirconia nanoparticles is presented in figure 1.

2.2a *Synthesis of zirconia by precipitation method (ZrO_2-P)*: 200 mL of double distilled water was adjusted to pH 9.0 by addition of liquid ammonia. To this solution required amount of zirconyl chloride solution was added drop wise under constant stirring. The pH of the solution was maintained at 9.0 by drop wise addition of ammonia solution. After completion of the precipitation process, the aqueous mixture was stirred for 6 h, filtered and washed multiple times with distilled water (till free from Cl^- ions). The precipitated materials was dried at 120°C for 12 h in a hot air oven and calcined at 450°C for 2 h to obtain the ZrO_2-P particles.

2.2b *Synthesis of zirconia by amorphous citrate method (ZrO_2-A)*: A solid mixture containing equimolar amount of zirconyl nitrate and citric acid was dissolved in minimum amount of water to form a thick paste. The paste was evacuated at 70°C to form an expanded hygroscopic solid which was immediately transferred to a hot air oven preheated at 160°C. The temperature of the oven was maintained at 160°C for 2 h to yield the amorphous citrate precursor. The amorphous precursor was calcined at 500°C for 2 h to obtain the ZrO_2-A particles.

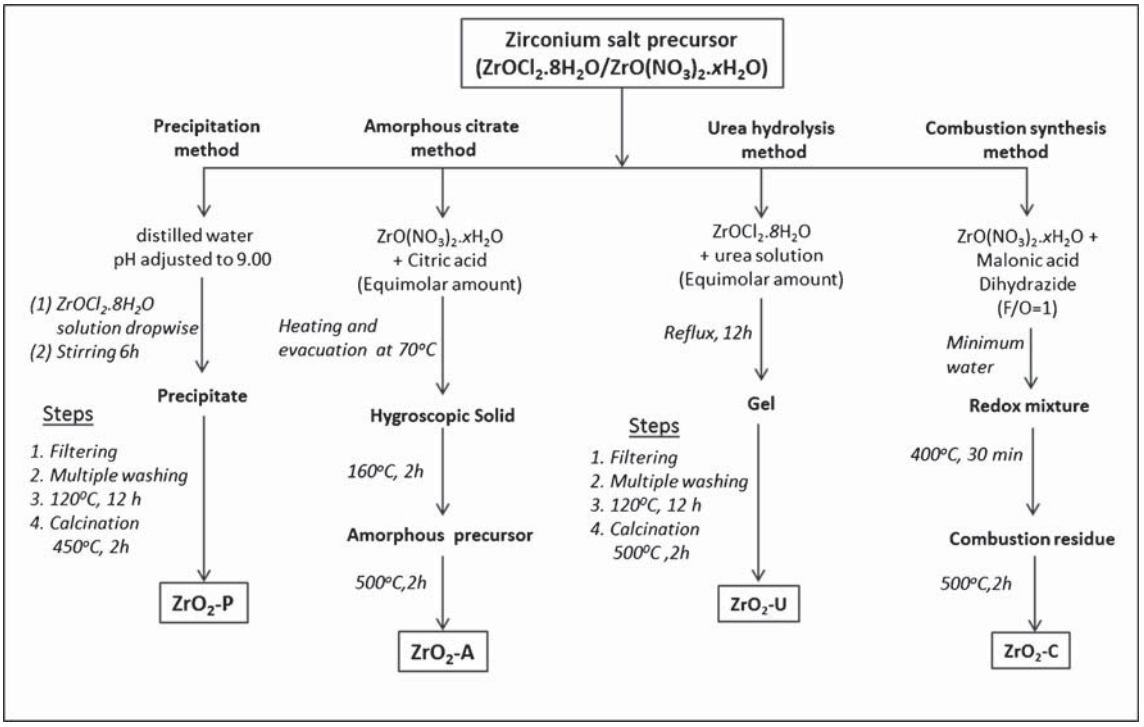

Figure 1. Synthetic schemes for preparation of zirconia nanoparticles.

2.2c *Synthesis of zirconia by urea hydrolysis method (ZrO_2-U)*: 200 mL of 0.2 M $ZrOCl_2$ solution was mixed with equimolar amount of urea solution and refluxed for 12 h at 100°C. The resulting solid material was filtered, washed repeatedly with hot water, dried at 120°C for 12 h in hot air oven and calcined at 500°C for 2 h to obtain the ZrO_2-U materials.

2.2d *Synthesis of zirconia by combustion synthesis method (ZrO_2-C)*: The zirconia nanoparticles were synthesized using malonic acid dihydrazide as fuel at a F/O stoichiometric ratio of 1. The F/O ratio was calculated using the method described by Jain *et al.*[34] Required amount of zirconyl nitrate and fuel was dissolved in minimum amount of water to obtain a redox mixture. The redox mixture was kept in a muffle furnace preheated at 400°C for 30 min. The redox mixture instantaneously gets ignited releasing a lot of gaseous products. The combustion residue is subsequently grinded and calcined at 500°C for 2 h in air to obtain the ZrO_2-C particles.

2.3 *Synthesis of Ba^{2+} modified zirconia nanoparticles (Ba/ZrO_2)*

In a typical procedure, 4 g of zirconia was dispersed in 50 mL of 10 mmol barium carbonate solution. The resulting suspension was stirred for 2 h, filtered and dried at 110°C for 6 h in a hot air oven. The obtained material was refluxed in 50 mL ethanol for 4 h, dried overnight at 120°C and calcined at 550°C for 2 h to generate the Ba/ZrO_2 materials.

2.4 *Characterization techniques*

The XRD patterns of the ZrO_2 and Ba/ZrO_2 nanomaterials were recorded using a Rigaku, Ultima-IV multipurpose X-ray diffraction system using Ni filtered $CuK\alpha_1$ ($\alpha = 1.5405$Å) radiation. The XRD measurements were carried out in the 2θ range of 20–70° with a scan speed of 2 degrees per minute using Bragg-Brantano configuration. The crystallite size has been calculated from the Fourier line profile analysis of the broadened XRD patterns following the Warren and Averbach method.[35] The Field emission scanning electron micrographs (FESEM) were taken using a Nova NanoSEM microscope model FEI operating at an acceleration voltage of 15 kV. Prior to FESEM analysis, the powder sample was placed on carbon tape followed by gold sputtering for three minutes. Transmission electron micrograph (TEM) of the Ba/ZrO_2 materials were recorded using JEM–2100 HRTEM equipment using carbon coated copper grids. The surface basic sites of Ba/ZrO_2 catalysts were estimated by non-aqueous titration method using the procedure reported elsewhere.[36] The specific surface area was determined by BET method using N_2 adsorption/desorption at 77K on an AUTOSORB 1 Quantachorme instrument. ^{1}H

NMR spectra were recorded with Bruker spectrometer at 400MHz using TMS as internal standard. Reactions were monitored by thin layer chromatography using 0.2 mm silica gel F-254 plates.

2.5 *Catalytic activity study*

2.5a *Catalytic activity for synthesis of β-nitro alcohols*: Typically, a reaction mixture containing p-nitro benzaldehyde (1 mmol), nitromethane (2 mmol) and 50 mg catalyst (Ba/ZrO_2-U) in 5mL of ethanol was stirred at different temperature for the specified time. After completion of the reaction as indicated by TLC, the catalyst particles were filtered and the products were extracted from the ethanolic solution. The crude product was recrystallized using acetonitrile to afford the β-nitro alcohol in 89% yield. The used catalyst particles were washed with ethyl acetate (3 times 5 mL portions) and calcined at 450°C for 2 h to regenerate the catalyst.

2.5b *Catalytic activity for synthesis of 2-amino 2-chromenes*: In a typical procedure, reaction mixture containing benzaldehyde (1 mmol), α-naphthol (1 mmol), malononitrile (1 mmol), and Ba/ZrO_2-U catalyst (50 mg) in PEG + water (2 mL, 1:1 molar ratio) was heated at 50°C for the required amount of time. After completion of the reaction, as indicated by TLC, the reaction mixture was diluted with water and the solid product was removed by filtration. The product was separated from catalyst by dissolving into hot methanol followed by simple filtration. The product was recovered from the methanolic solution and recrystallized from ethyl acetate to afford the pure product in 84% yield.

All β-nitro alcohols and 2-amino 2-chromenes synthesized in this work are known compounds and are identified by comparing their physical and spectral characteristics with literature.[18–33]

3. Results and Discussion

3.1 *Characterization of the Ba/ZrO_2 nanoparticles*

The XRD patterns of the zirconia samples prepared by different methods are presented in figure 2. All zirconia materials exhibited well-defined and intense characteristic reflections with d spacing values of 3.15, 2.95. 2.83, 2.57, 2.50, 1.83, 1.80, 1.55 and 1.53 Å. These peaks correspond to the presence of both monoclinic and tetragonal phase of zirconia (JCPDS-ICDD file no. 83–0940 and 81–1545). The percentage of tetragonal phase present in each sample was calculated using the literature reported method.[37] The relative content of monoclinic and tetragonal phases of the zirconia samples depend strongly on the method of preparation.

The ZrO_2-A sample prepared by amorphous citrate process contain 96% tetragonal phase whereas the combustion synthesized zirconia material contains 69.4% tetragonal phase (table 1).

The difference in the tetragonal phase content can be related to the crystallite size of these samples. The stabilization of the tetragonal phase in zirconia sample has

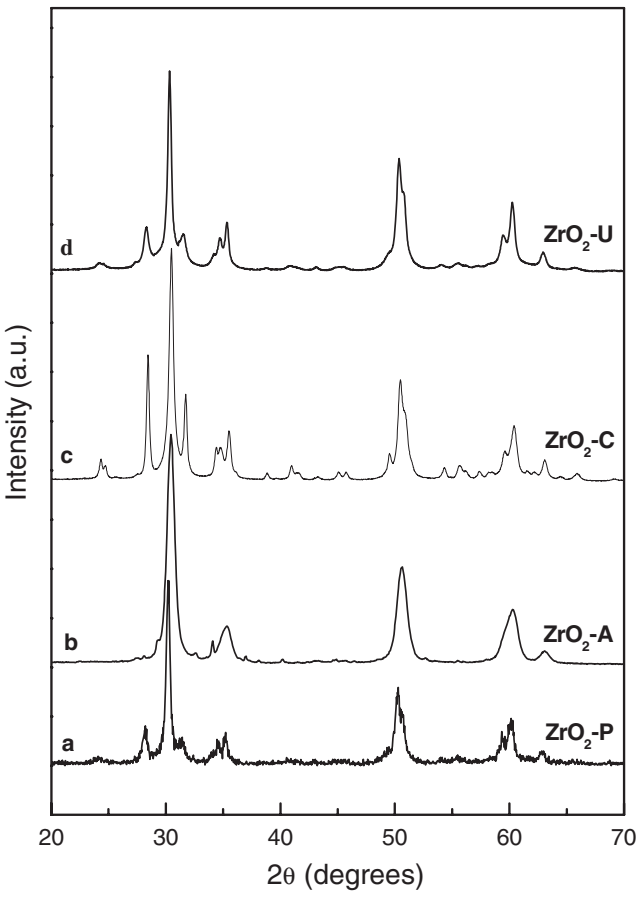

Figure 2. XRD patterns of (a) ZrO_2-P, (b) ZrO_2-A, (c) ZrO_2-C and (d) ZrO_2-U materials.

Table 1. Percentage tetragonal phase and crystallite size of the zirconia and Ba/ZrO_2 materials.

Material	% tetragonal phase	Crystallite size (nm)[a]
ZrO_2-U	83.3	7.2
ZrO_2-A	96.0	5.0
ZrO_2-C	69.4	9.1
ZrO_2-P	82.1	18.6
Ba/ZrO_2-U	100	9.4
Ba/ZrO_2-A	100	7.5
Ba/ZrO_2-C	78.8	12.6
Ba/ZrO_2-P	100	22.0

[a]Calculated from the Fourier analysis of the broadened XRD profile.

been a subject of intense study in literature.[38–43] The tetragonal phase being metastable in nature undergoes a martensitic transformation to the monoclinic phase.[41] The presence of aliovalent impurities in zirconia structure as well as surface modification by ionic species selectively stabilizes the tetragonal phase.[40–43] The aliovalent dopants such as Fe^{3+} ions induce oxygen ion vacancy in the zirconia lattice which in turn helps in the stabilization of tetragonal phase.[41,43] The surface modification process on the other hand reduces the grain boundary area among the zirconia particles preventing the mobility of ions during phase transformation.[42] It has also been reported that there is a critical crystallite size of zirconia below which the tetragonal phase is stabilized.[39,44] In the present study it is believed that the crystallite size is the key factor which controls the tetragonal phase stabilization. In order to verify this proposition, the Fourier line profile analysis of the broadened XRD peaks are carried out following the Warren and Averbach method[35] using software BRAEDTH[45] The calculated volume-weighted distributions (PV), and Fourier size coefficient (AS) as function of Fourier length (L) is presented in figure 3.

As observed from figure 3 I, the volume weighed crystallite distribution for ZrO_2-U and ZrO_2-C and ZrO_2-A are quite narrow whereas the distribution function spread over a wide range in case of ZrO_2-P material. The average crystallite size calculated from figure 3 II is presented in table 1. There seems to be a direct correlation between the crystallite size and the percentage of tetragonal phase content in the sample. The zirconia material prepare using combustion, amorphous citrate and urea hydrolysis method contains crystallites with size less than 10 nm whereas the zirconia synthesized by precipitation method display higher average crystallite size. The XRD patterns of the Ba/ZrO_2 materials are presented in figure 4. The characteristics XRD peaks corresponding to tetragonal phase of zirconia is only observed for Ba/ZrO_2-A, Ba/ZrO_2-U and Ba/ZrO_2-P materials. However, the Ba/ZrO_2-C material contains a mixture of monoclinic and tetragonal phases. In addition to the XRD peaks corresponding to tetragonal zirconia lattice, less intense and broad peaks are observed at 2θ values of 27.8, 28.3, 39.8, 42.5, 45.1 and 47.3 degrees. These peaks correspond to the presence of a minor amount of $BaCO_3$ and BaO phases in the Ba/ZrO_2 samples (JCPDS-ICDD files no. 78-2057 and 22-1056, respectively).

In the presence of Ba^{2+} ions, the selective stabilization of the tetragonal phase of zirconia is quite effective for all ZrO_2 materials except for the combustion synthesis samples. As discussed earlier, the surface modification by ionic species lead to a reduction in the grain boundary area between adjacent zirconia grains. The reduction in grain boundary area prevents tetragonal to monoclinic phase transitions. The selective stabilization of the tetragonal phase in the present study can be ascribed to the presence of well-dispersed Ba species on zirconia surface. The amount of barium ions present on the zirconia surface is estimated using EDAX analysis (table 2). It is observed that the uptake of barium ions is strongly dependent on the method of synthesis. The Ba^{2+} ions are grafted onto the surface of zirconia primarily through interaction with the surface hydroxyl groups, the relative amount of which depends on the method of synthesis.

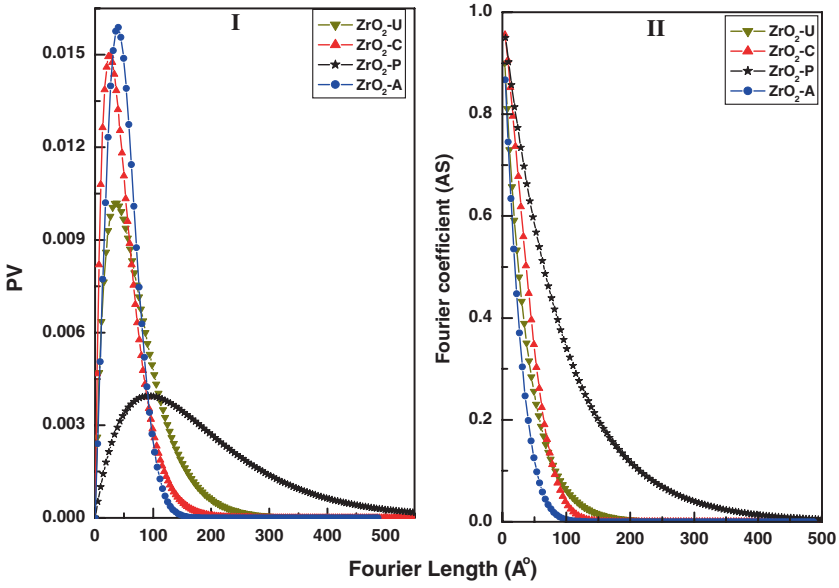

Figure 3. Fourier analysis plots for ZrO_2 nanoparticles (PV∼L, Panel I and AS∼L Panel II).

In case ZrO_2-C sample, since the combustion process is highly exothermic with adiabatic reaction temperature crossing 1273 K, at this temperature most of the surface hydroxyl groups are destroyed leading to the poor uptake of barium (table 2). The Fourier plots for the Ba/ZrO_2 materials are presented in figure 5.

Compared to pure zirconia samples, the Ba/ZrO_2 materials exhibit broad distribution functions which extend up to the Fourier length of 50 nm. The size distribution of the crystallites increases in the order Ba/ZrO_2-A ≈ Ba-ZrO_2-U <Ba/ZrO_2-C<Ba/ZrO_2-P. The average crystallite size calculated from figure 5b is presented in table 1. The average crystallite size is found to be higher in case of Ba/ZrO_2 sample as compared to the pure zirconia samples probably due to the surface growth occurred during the surface grafting process.

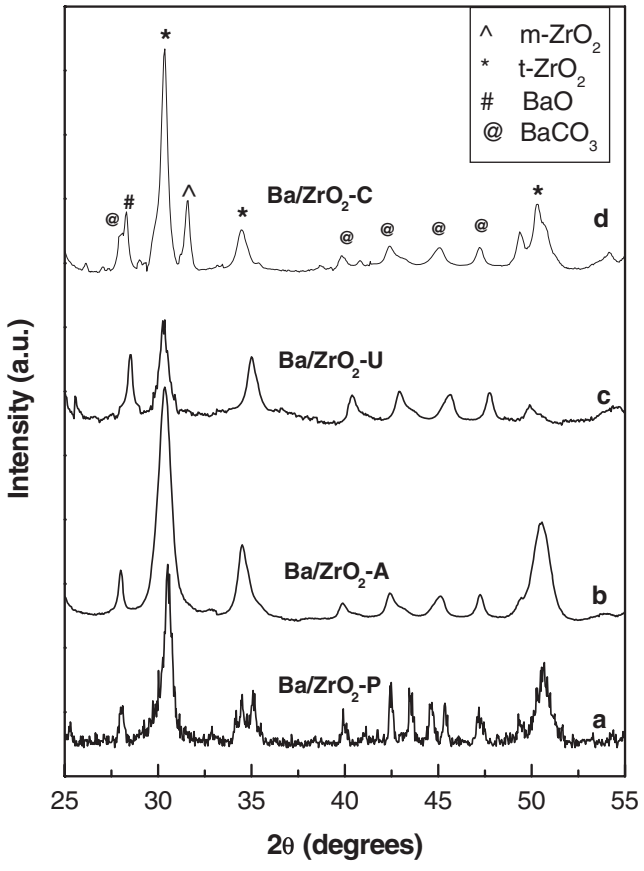

Figure 4. XRD patterns of (a) Ba/ZrO_2-P, (b) Ba/ZrO_2-A, (c) Ba/ZrO_2-U and (d) Ba/ZrO_2-C.

The UV-Vis-DRS spectra of the zirconia sample along with Ba/ZrO_2 materials are presented in figure 6. Pure ZrO_2 prepared by different methods shows a sharp and intense band at 214 nm with an absorption edge around 350 nm. ZrO_2 is a direct band gap insulator which shows an interband transition in the UV region of the spectrum.[41–43] The monoclinic form of ZrO_2 has two direct interband transitions at 5.93 and 5.17 eV, whereas the tetragonal form has a band gap of 5.1 eV.[41] In the present case, the peak at 214 nm can be assigned to the $O^{2-} \rightarrow Zr^{4+}$ charge transfer transition arising from the host zirconia matrix (figure 6 I).[41]

The Ba/ZrO_2 materials exhibit similar absorption feature as that of pure zirconia samples. However, the absorption edge is red shifted and appear at $\lambda > 400$ nm. The red shifting of the absorption edge in presence of Ba^{2+} ions can be ascribed to the structural disorder in zirconia lattice. The presence of structural disorder and defect centers shifts the adsorption edge to higher wavelength due to the presence of localized states between the valence and conduction band edges.

The field emission scanning electron micrograph of the Ba/ZrO_2 materials are presented in figure 7. The morphology of the Ba/ZrO_2 materials depends strongly on the method of synthesis. The Ba/ZrO_2-A and Ba/ZrO_2-C materials contain particles of different size with flake-like morphology (figure 7a and 7b). The particles are present in a highly agglomerated state. Both Ba/ZrO_2-A and Ba/ZrO_2-C materials are of low density and spongy in nature.

The similarity in their morphological characteristics is related to the exothermic decomposition route by which both samples have been synthesized. In the amorphous citrate process, the amorphous precursor contains hydroxycitrates of the metal ions which decompose exothermically at higher temperature to yield the metal oxide.[5] Similarly, in the combustion synthesis method the exothermic decomposition of the fuel is responsible for conversion of salt precursor to the metal oxide.[37] In both the methods, large amount of gaseous products

Table 2. Physicochemical properties and catalytic activity of the Ba/ZrO_2 catalyst.

Material	Barium content[a] (atom%)	Surface area (m^2/g)	Basic sites[b] (mmol/g)	Yield[c] (%)	Time (h)	Rate[d] (mmol $h^{-1}g^{-1}$)	Rate (mmol h^{-1} m^{-2}x 10^{-3})
Ba/ZrO_2-U	6.68	56.2	0.48	89.0	2.5	7.2	6.4
Ba/ZrO_2-A	4.13	65.1	0.42	75.0	3.0	5.2	4.0
Ba/ZrO_2-C	2.16	29.4	0.38	62.8	4.0	3.2	5.5
Ba/ZrO_2-P	3.85	35.6	0.35	58.6	4.0	3.0	4.2

[a]Obtained from EDAX analysis. [b]Estimated from non-aqueous titration method. [c]Refers to pure and isolated yield. [d]Calculated by estimating the benzaldehyde conversion in the reaction mixture by GC analysis.

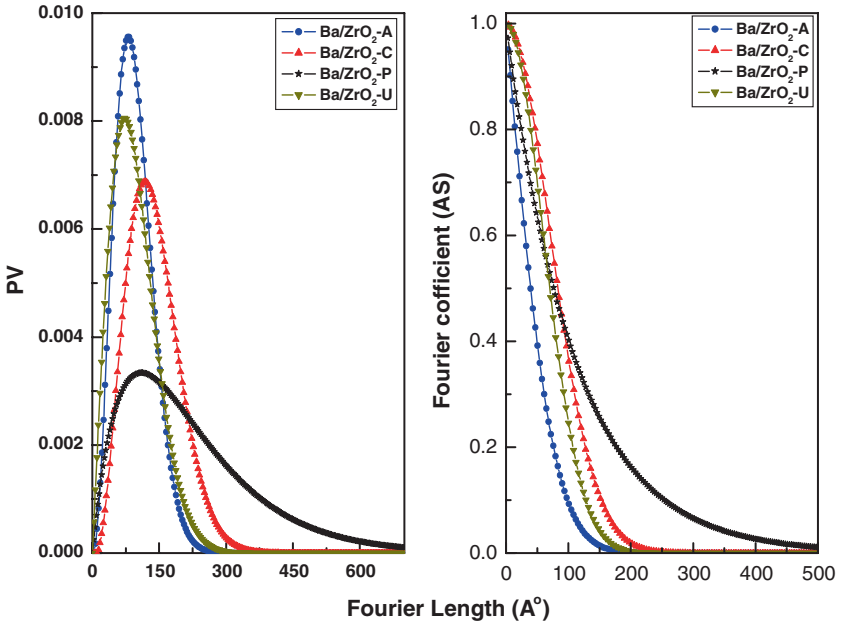

Figure 5. Fourier analysis plots for Ba/ZrO_2 materials (PV∼L, Panel I and AS∼L Panel II).

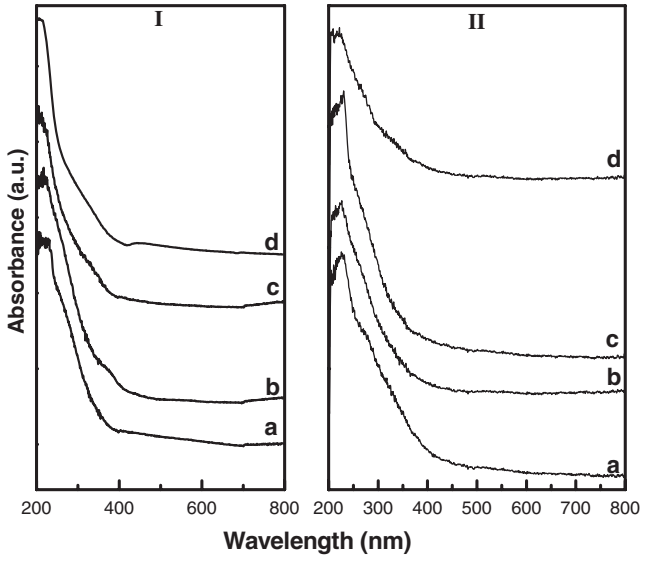

Figure 6. UV-Vis-DRS spectra of (a) ZrO_2-U, (b) ZrO_2-A, (c) ZrO_2-C, (d) ZrO_2-P (Panel I) and (a) Ba/ZrO_2-U, (b) Ba/ZrO_2-A, (c) Ba/ZrO_2-C, (d) Ba/ZrO_2-P (Panel II).

are formed due to the exothermic decomposition reaction which leaves the material porous and spongy. The Ba/ZrO_2-P material contains particles of irregular shapes and sizes without any attributed morphology. In contrast to this observation, the Ba/ZrO_2-U material contains numerous small spherical particles in an agglomerated state. The TEM images of the Ba/ZrO_2 materials are presented in figure 8.

The Ba/ZrO_2-U material contains crystallites with size in the range of 8-10 nm. The presence of two different phases with clear contrast can be observed from TEM image (figure 8a). The $BaCO_3$/BaO phase is present in a well-dispersed state in the ZrO_2 matrix. There is a considerable mismatch along the grain boundary region as observed from the high magnification image (figure 8b). The Ba/ZrO_2-A and Ba/ZrO_2-C materials also contain spherical particles with size in the range of 10-15 nm (figure 8c and d). The Ba/ZrO_2-P material, on the other hand, contains agglomerated particles without well-defined shape. The observed particle size range is 20-40 nm for Ba/ZrO_2-P materials, which is significantly higher than the other Ba/ZrO_2 materials prepared in this work.

3.2 *Catalytic activity study*

3.2a *β-nitro alcohol synthesis*: The catalytic activity of the Ba/ZrO_2 material is evaluated for the synthesis of β-nitro alcohols by condensation of aryl aldehydes with nitromethane in ethanol solvent (scheme 1). Initially, the condensation of 4-nitro benzaldehyde and nitromethane is taken as a model reaction and different Ba/ZrO_2 materials are studied for their catalytic activity. The surface properties, barium content and catalytic activity of the Ba/ZrO_2 materials are presented in table 2.

Among the different Ba/ZrO_2 studied in this work, the Ba/ZrO_2-U material exhibit highest catalytic activity providing 89% yield of the product after 2.5 h of reaction time at 40°C. This catalyst also exhibits higher amount of barium retention on its surface and more number of basic sites among the Ba/ZrO_2 materials. The surface area of the Ba/ZrO_2 materials is presented in table 2. The Ba/ZrO_2 sample prepared by amorphous citrate method and urea hydrolysis method exhibit

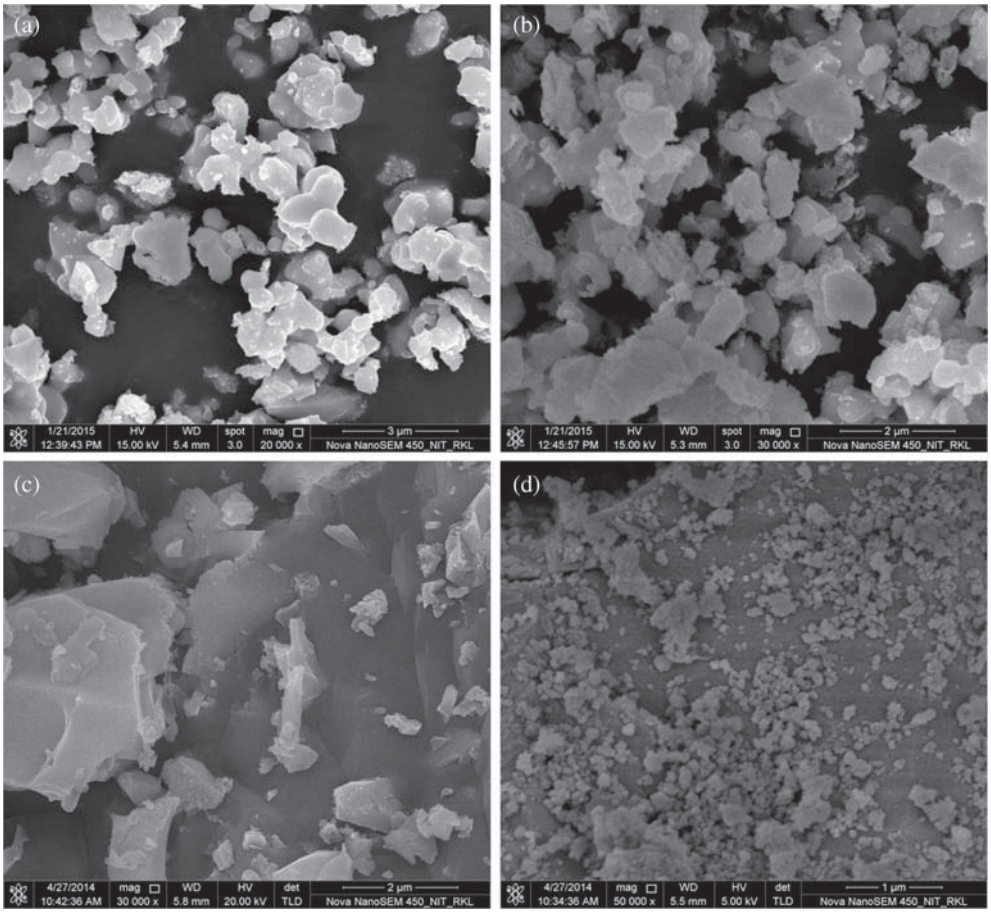

Figure 7. FESEM images of (a) Ba/ZrO_2-A, (b) Ba/ZrO_2-C, (c) Ba/ZrO_2-P and (d) Ba/ZrO_2-U.

comparable but higher surface area compared to the Ba/ZrO_2-P and Ba/ZrO_2-C samples. The surface area and barium retention is strongly influenced by the preparative method used for zirconia synthesis. Since the Ba/ZrO_2 materials exhibit different surface areas and basicity, for comparison purpose, the reaction rates are calculated in terms of unit surface area and mass of the catalyst by estimating the conversion of 4-nitrobenzaldehyde in the reaction mixture by GC analysis (table 2). Among the Ba/ZrO_2 catalysts, the Ba/ZrO_2-U catalyst shows higher reaction rates as compared to other materials. Based on the results described in table 2, the Ba/ZrO_2-U catalyst is selected for further studies. The reaction parameters were optimized by varying catalyst amount, reaction stoichiometry, reaction media and temperature It was observed that for a reaction involving 1 mmol of the arylaldehyde, 50 mg of the catalyst is ideal for an efficient condensation of the reactants. The optimum reactant ratio was found to be 1:2 for 4-nitrobenzaldehyde and nitromethane, respectively. The effect of reaction media on the catalytic activity was studied by employing solvents with different polarity in the reaction protocol (figure 9 I).

It is noticed that for nonpolar solvents such as hexane the yield of the product is very less. The yield is found to improve upon use of polar solvent. The less yield observed in aqueous medium can be attributed to the limited solubility of the reactants in water. Among different solvent tried for the reaction, better yield is observed when ethanol is employed as a reactant. Hence ethanol is used as a solvent for further study. The effect of reaction temperature is studied by varying the temperature in the range of 30–50°C. With an increase in the temperature the yield of β-nitro alcohol (table 3, Entry 2) increases significantly up to 40°C. Further increase in temperature to 50°C marginally improves the yield (figure 9 II). Hence in this study, the reaction temperature is fixed at 40°C. Ensuing optimized conditions for the β-nitro alcohol synthesis, we explored the scope and limitations of the optimized protocol by using different substituted aromatic aldehydes (table 3).

It was observed that the aromatic aldehydes containing electron withdrawing groups react faster in the optimized protocol as compared to the aldehydes with electron donating groups. However, a variety of substituted aldehydes reacted in the optimized protocol to yield the corresponding β-nitro alcohols in high yield and purity. The recyclability of the Ba/ZrO_2-U catalyst was tested for three consecutive cycles taking the condensation of 4-nitro benzaldehyde and nitromethane

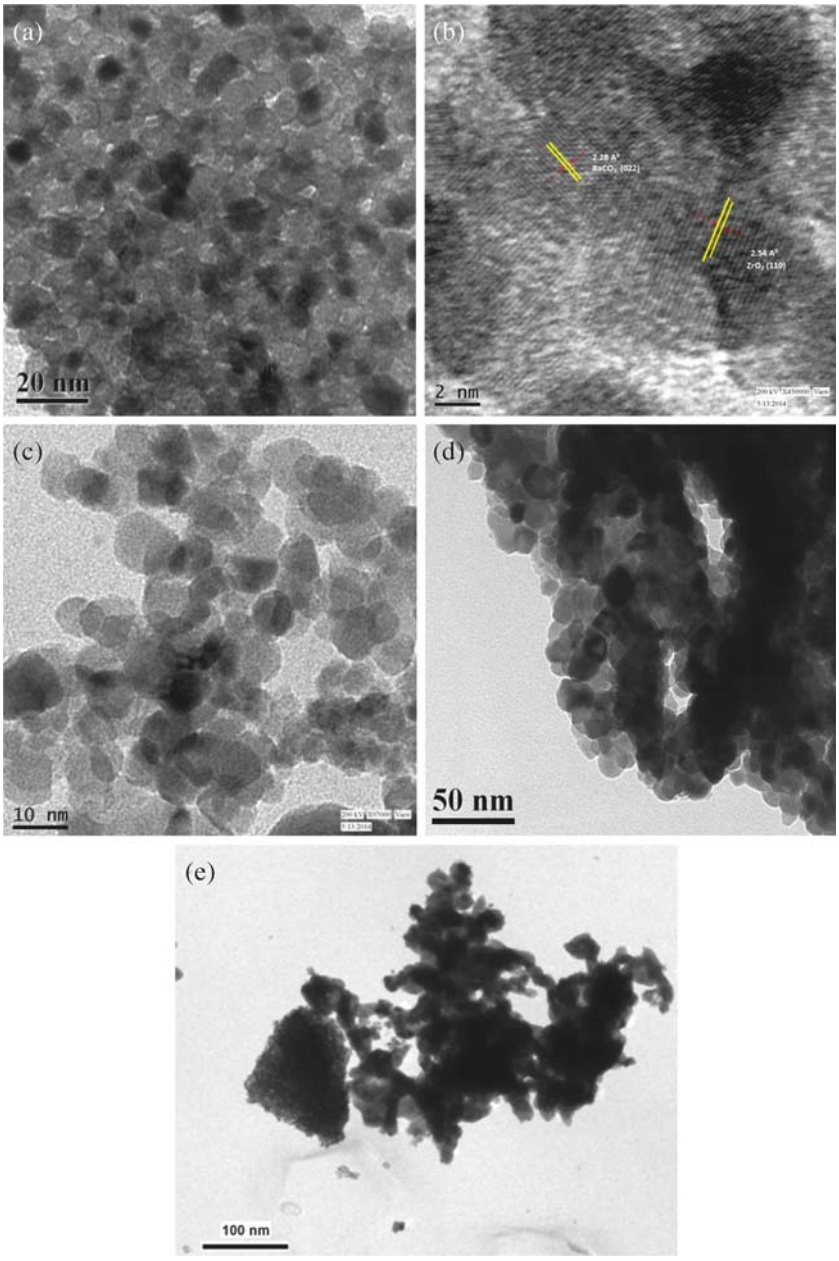

Figure 8. Transmission electron micrograph of (a) Ba/ZrO_2-U, (b) Ba/ZrO_2-U with higher magnification, (c) Ba/ZrO_2-A, (d) Ba/ZrO_2-C, (e) Ba/ZrO_2-P materials.

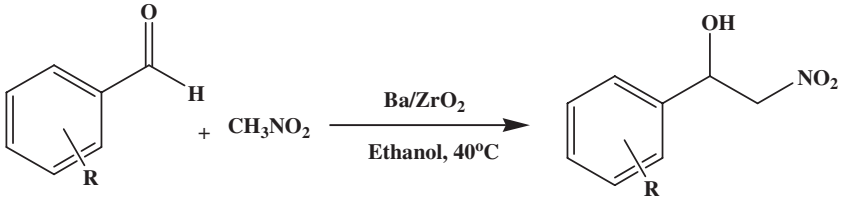

Scheme 1. Ba/ZrO_2 catalyzed condensation of aryl aldehydes with nitromethane.

as a model reaction under optimized reaction conditions. After completion of each cycle, the catalyst particles were filtered, washed with 10 mL of ethyl acetate and dried in hot air oven. The catalyst particles were regenerated by heat treatment at 450°C for 2 h. The Ba/ZrO_2-U catalyst could be recycled upto three

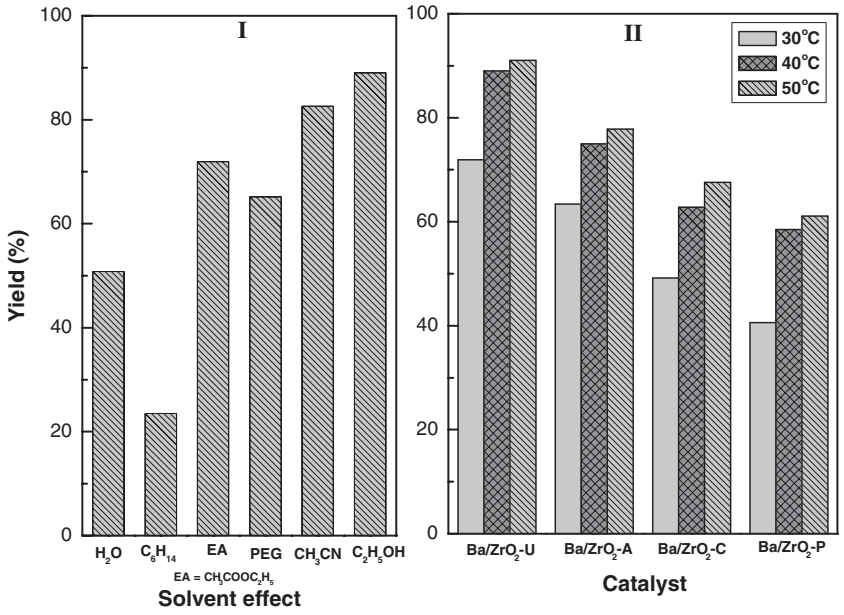

Figure 9. Effect of reaction media (I) and temperature (II) on the yield of β-nitro alcohol (table 3, entry 2).

Table 3. Ba/ZrO_2-U catalyzed synthesis of structurally diverse β-nitro alcohols.

Sl. No.	R	Time (h)	Yield (%)
1	H	3.0	78.0
2	4-NO_2	2.5	89.0
3	4-OCH_3	4.0	76.0
4	4-OH	4.0	82.0
5	2-OH	4.0	80.0
6	3-NO_2	3.0	86.5
7	2-NO_2	2.5	93.0
8	4-Cl	3.0	87.6
9	4-F	4.0	81.5

consecutive cycles without any significant loss in the catalytic activity (table 3, Entry 2, yields, 89%, 1st; 86%, 2nd; 84%, 3rd).

3.2b *Synthesis of 2-amino-2-chromenes*: The catalytic activity of the Ba/ZrO_2-U catalyst is further explored for synthesis of 2-amino-2-chromenes by multicomponent one pot condensation of aryl aldehydes, malononitrile, and α-naphthol (scheme 2).

Initially, the condensation of benzaldehyde, malononitrile and α-naphthol was taken as a model reaction and the reaction parameters are optimized by varying the catalyst amount, temperature, reaction media and molar ratio of the reactants. For reaction involving 1 mmol of the reactants, 50 mg of the Ba/ZrO_2-U catalyst was ideal for efficient condensation of the three components to afford the corresponding 2-amino-2-chromenes in 84% yield (table 4, Entry 1). Further increase in the catalyst amount does not lead to an appreciable increase in yield of the product. The reaction temperature was varied between 40-80°C. At 50°C, significant yield of the product was observed which does not improve substantially upon further increase in temperature. The optimum reactant ratio is found to be 1:1:1 for benzaldehyde, malononitrile and α-naphthol, respectively. The effect of reaction media was studied by using solvents with different polarity under the optimized reaction condition. The product yield was found to improve in the presence of polar solvent as compared to the nonpolar solvents. The best yield of the product was attained when PEG + water in 1:1 molar ratio was used as solvent. Ensuing optimized condition for the multicomponent condensation, we explored the scope and limitation of the catalytic protocol by using different substituted aromatic aldehydes (table 4). Under identical reaction conditions, aryl aldehydes bearing electron withdrawing and donating groups reacted efficiently to give the corresponding 2-amino-2-chromenes in high yield and purity. Recyclability study of Ba/ZrO_2-U material was carried out upto three catalytic cycles for synthesis of 2-amino-2-chromene (table 4, Entry 1) using the procedure described in section 3.2a. No significant decrease in yield of the product was observed in recyclability study (table 4, Entry 1, yields, 84%, 1st; 82%, 2nd; 78%, 3rd) indicating the stable activity of the Ba/ZrO_2-U catalyst for synthesis of 2-amino 2-chromenes.

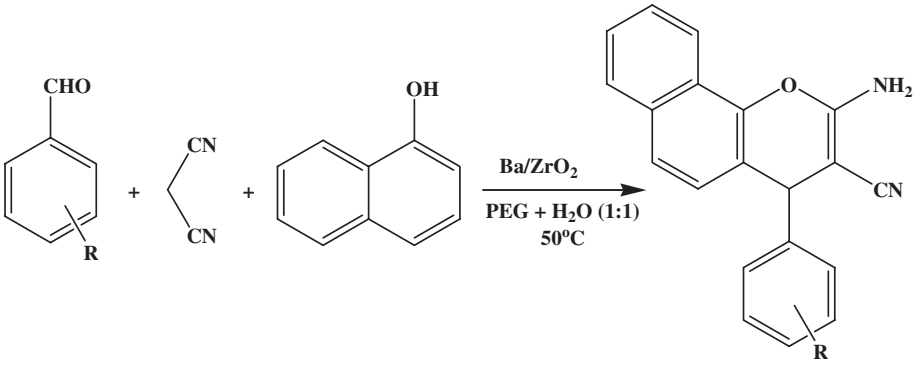

Scheme 2. Ba/ZrO_2 catalyzed synthesis of 2-amino 2-chromene.

Table 4. Ba/ZrO_2-U catalyzed synthesis of 2-amino 2-chomenes.

Sl. No.	R	Time (min)	Yield (%)
1	H	120	84
2	4-Cl	150	82
3	2-Cl	150	81
4	4-OCH_3	120	89
5	4-NO_2	120	86
6	3-NO_2	120	88
7	2-NO_2	150	80
8	4-Br	150	79
9	4-F	180	76

4. Conclusions

In this work, we have prepared Ba^{2+} ion grafted zirconia nanoparticles by employing zirconia particles synthesized by different methods. The selective stabilization of the tetragonal phase of zirconia was observed for the Ba/ZrO_2 samples. The presence of $BaCO_3$ and BaO as minor phase is also detected from XRD study. The Ba/ZrO_2 samples exhibit particle size in the range of 9-25 nm depending upon the method adopted for synthesis of ZrO_2 particles. The Ba modified zirconia nanoparticles exhibit high surface area and surface basicity. The barium content on the surface strongly depends on the method of synthesis. The Ba/ZrO_2-U material was used as an efficient heterogeneous base catalyst for synthesis of β-nitro alcohols and 2-amino 2-chromenes. Both classes of materials were synthesized in high yield and purity using the Ba/ZrO_2 catalyst. The protocol developed in this work is advantageous in terms of simple experimentation, preclusion of toxic solvents, less reaction time, recyclability of catalyst, high yield and high purity of the products.

Acknowledgements

We would like to thank Board of Research in Nuclear Sciences (BRNS), Mumbai for financial support.

References

1. Ono Y and Hattori H 2012 In *Solid Base Catalysis* (Germany: Springer Verlag)
2. Busca G 2010 *Chem. Rev* **110** 2217
3. Corma A and Iborra S 2006 *Adv. Catal.* **49** 239
4. Kumar D, Mishra B G, Reddy V B, Rana R K and Varma R S 2007 *Tetrahedron* **63** 3093
5. Samantaray S, Pradhan D K, Hota G and Mishra B G 2012 *Chem. Eng. J.* **193** 1
6. Urbano F J, Aramendía M A, Marinas A and Marinas J M 2009 *J. Catal.* **268** 79
7. Zhang Q, Zhang Y, Li H, Gao C and Zhao Y 2013 *Appl. Catal. A* **466** 233
8. Choudhary V R and Karmakar A J 2003 *Proc. Indian Acad. Sci. (J. Chem. Sci.)* **115** 281
9. Ranga Rao G and Sahu H R 2001 *Proc. Indian Acad. Sci. (J. Chem. Sci.)* **113** 651
10. Tian X, Zeng Y, Xiao T, Yang C, Wang Y and Zhang S 2011 *Micropor. Mesopor. Mater.* **143** 357
11. Shen W, Tompsett G A, Hammond K D, Xing R, Dogan F, Grey C P, Conner W C, Auerbach S M and Huber G W 2011 *Appl. Catal. A* **392** 57
12. Eta V, Arvela P M, Wärnå J, Salmi T, Mikkol J and Murzin D 2011 *Appl. Catal. A* **404** 39
13. Xia S, Guo X, Mao D, Shi Z, Wu G and Lu G 2014 *RSC Adv* **4** 51
14. Zhang Q, Zhang Y, Li H, Gao C and Zhao Y 2013 *Appl. Catal. A* **233** 239
15. Wang C, Sun N, Kang M, Wen X, Zhao N, Xiao F, Wei W, Zhaod T and Sun Y 2013 *Catal. Sci. Tech.* **3** 2435
16. Gong L, Sun L, Sun Y, Li T and Liu X 2011 *J. Phys. Chem. C* **115** 11633
17. Hamad B, Perard A, Figueras F, Prakash S and Essayem N 2010 *J. Catal.* **269** 1
18. Luzzio F A 2001 *Tetrahedron* **57** 915
19. Bures J and Vilarrasa J 2008 *Tetrahedron Lett.* **49** 441
20. Ren Y and Cai C 2007 *Catal. Lett.* **118** 134
21. Wang Q and Shantz D F 2010 *J. Catal.* **271** 170
22. Biradar A V, Sharma K K and Asefa T 2010 *Appl. Catal. A* **389** 19
23. Dhahagani K, Rajesh J, Kannan R and Rajagopal G 2011 *Tetrahedron Asym.* **22** 857
24. Kidwai M, Saxena S, Khan M K R and Thukral S S 2005 *Bioorg. Med. Chem. Lett.* **15** 4295
25. Majumdar N, Paul N D, Mandal S, Bruin B de and Wulff W D 2015 *ACS Catal.* **5** 2329

26. Varma R S and Dahiya R 1998 *J. Org. Chem.* **63** 8038
27. Solhy A, Elmakssoudi A, Tahir R, Karkouri M, Larzek M, Bousmina M and Zahouily M 2010 *Green Chem.* **12** 2261
28. Golari N, Rahimizadeh M, Bakavoli M and Rezaei-Seresht E 2015 *Res. Chem. Intermed.* **41** 6023
29. Ballini R, Bosica G, Conforti M L, Maggi R, Mazzacani A, Righic P and Sartori G 2001 *Tetrahedron* **57** 1395
30. Gong K, Wang H L, Fang D and Liu Z L 2008 *Catal. Commun.* **9** 650
31. Chen L, Huang X J, Li Y Q, Zhou M Y and Zheng W J 2009 *Monatsh. Chem.* **140** 45
32. Zhen Y, Lin H, Wanga S and Tao M 2014 *RSC Adv.* **4** 26122
33. Sangsuwan R, Sanger S, Aree T, Mahidol C, Ruchirawatabd S and Kittakoop P 2014 *RSC Adv.* **4** 13708
34. Jain S R, Adiga K C and Verneker V R 1981 *Combust. Flame* **40** 71
35. Warren B E and Averbach B L 1950 *J. Appl. Phys.* **21** 595
36. Ranga Rao G, Sahu H R and Mishra B G 2003 *React. Kinet. Catal. Lett.* **78** 151
37. Samantaray S, Mishra B G, Pradhan D K and Hota G 2011 *Ceram. Int.* **37** 3101
38. Figueroa S, Desimoni J, Rivas P C, Cervera M M and Caracoche M C 2005 *Chem. Mater.* **17** 3486
39. Chang S M and Doong R N 2005 *Chem. Mater.* **17** 4837
40. Chen L, Hu J and Richards R M 2008 *Chem. Phys. Chem.* **9** 1069
41. Navío J A, Hidalgo M C, Colón G, Botta S G and Litter M I 2001 *Langmuir* **17** 202
42. Samantaray S and Mishra B G 2011 *J. Mol. Catal. A: Chem.* **339** 92
43. Pradhan S and Mishra B G 2015 *RSC Adv.* **5** 86179
44. El-Sharkawy E A, Khder A S and Ahmed A I 2007 *Micropor. Mesopor. Mater.* **102** 128
45. Balzar D and Ledbetter H 1993 *J. Appl. Crystallogr.* **26** 97